Supporting Information

Insights into mechanisms of diphosphine-mediated controlled surface construction on Au nanoclusters

Qinzhen Li,[a] Sha Yang,[b] Jinsong Chai,[b] Hui Zhang*[a] and Manzhou Zhu*[b]

[a] School of Materials Science and Engineering, Anhui University, Hefei, Anhui 230601, China.

[b] Department of Chemistry and Centre for Atomic Engineering of Advanced Materials, Key Laboratory of Structure and Functional Regulation of Hybrid Materials of Ministry of Education, Institutes of Physical Science and Information Technology and Anhui Province Key Laboratory of Chemistry for Inorganic/Organic Hybrid Functionalized Materials, Anhui University, Hefei, Anhui 230601, China.

1. Supporting Figures

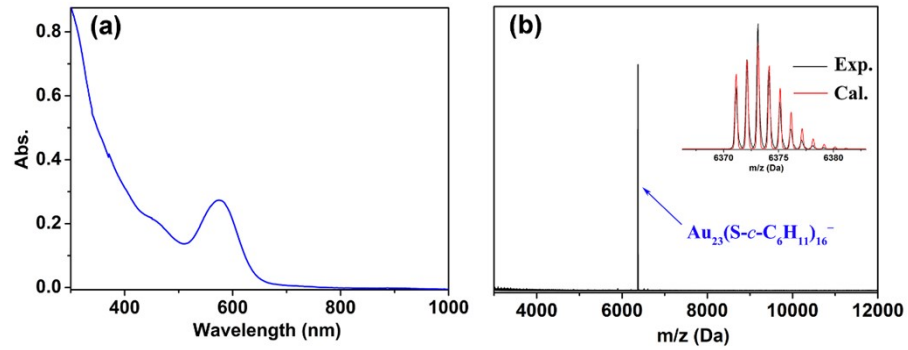

Fig. S1 (a) UV-vis spectrum and (b) ESI-MS of $Au_{23}(SR)_{16}^-$. Inset shows the experimental (black) and calculated (red) isotopic patterns of the main peak.

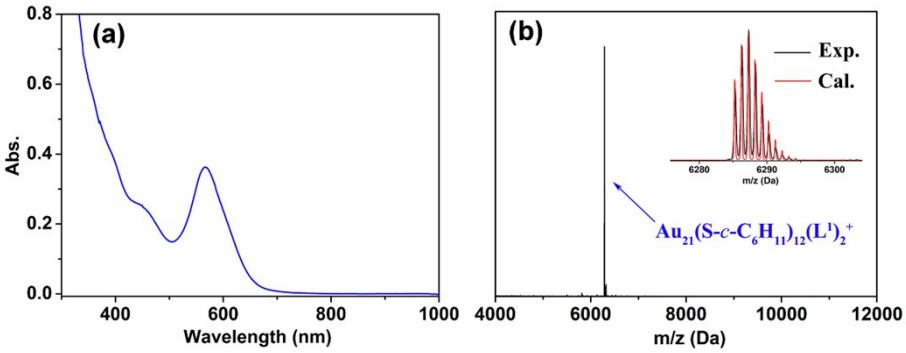

Fig. S2 (a) UV-vis spectrum and (b) ESI-MS of **Au_{21}-L^1**. Inset shows the experimental (black) and calculated (red) isotopic patterns of the main peak.

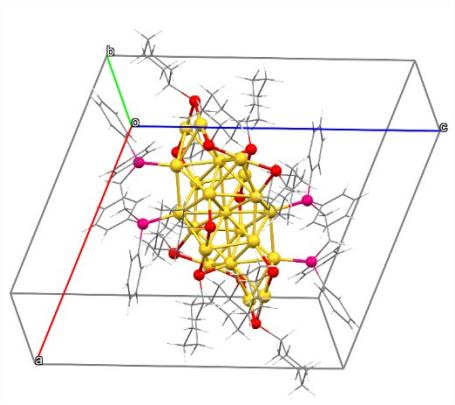

Fig. S3 A unit cell of the **Au_{21}-L^2** crystal. (Labels: golden = Au; red = S; magenta = P; gray = C; white = H.)

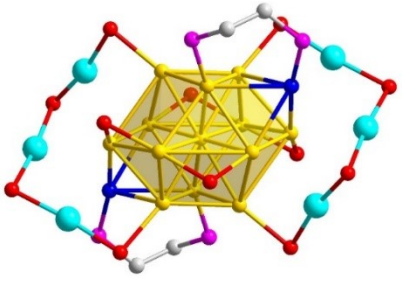

Fig. S4 Crystal structure of **Au_{21}-L^2**. All of the H atoms and most of the carbon atoms are omitted. (Labels: sky blue, blue, golden = Au; red = S; magenta = P; gray = C.)

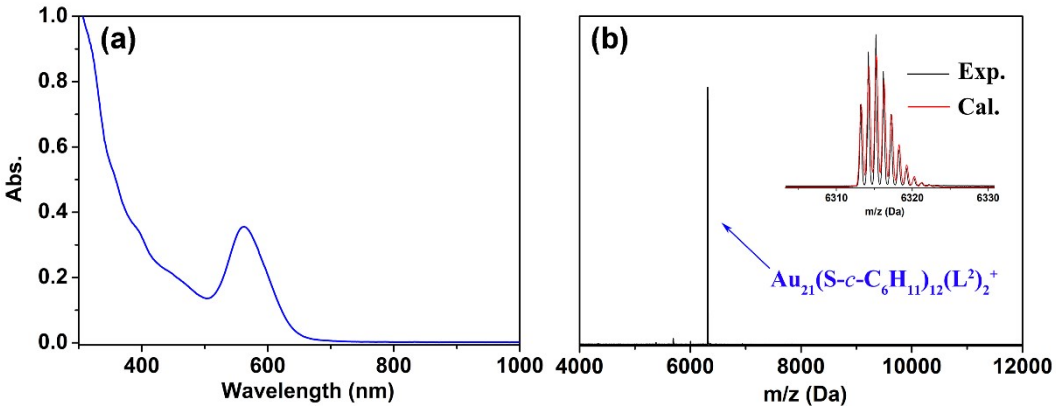

Fig. S5 (a) UV-vis spectrum and (b) ESI-MS of **Au_{21}-L^2**. Inset shows the experimental (black) and calculated (red) isotopic patterns of the main peak.

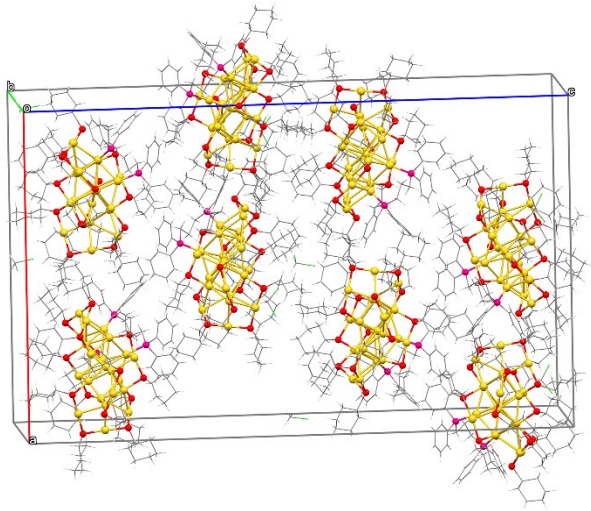

Fig. S6 A unit cell of the **Au_{22}-L^3** crystal. (Labels: golden = Au; red = S; magenta = P; green = Cl; gray = C; white = H.)

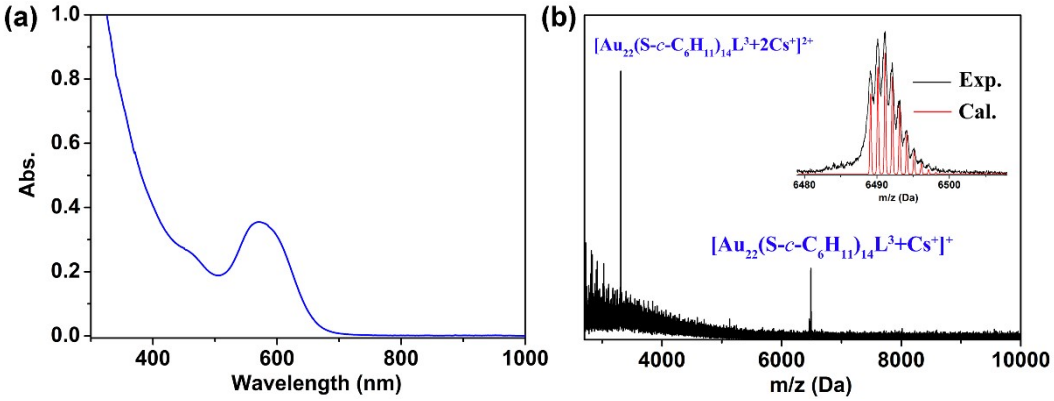

Fig. S7 (a) UV-vis spectrum and (b) ESI-MS of **Au_{22}-L^3**. Inset shows the experimental (black) and calculated (red) isotopic patterns of the main peak. CsOAc was added to enhance the ionization of the neutral nanoclusters.

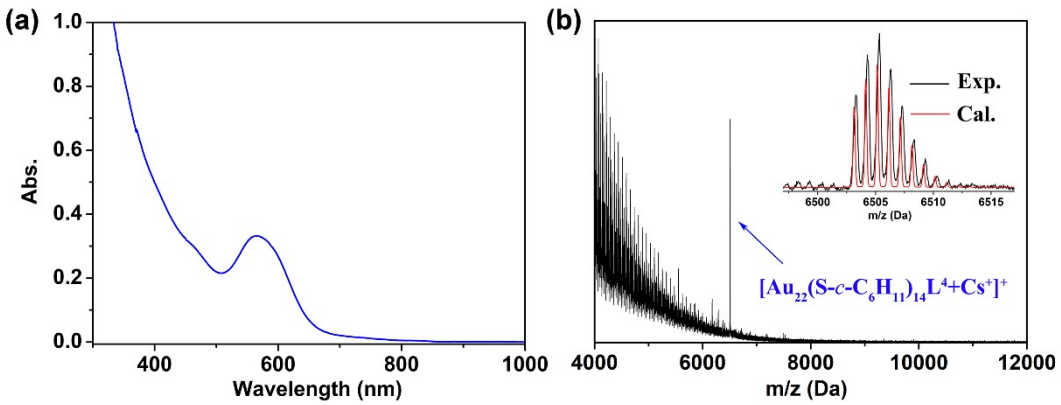

Fig. S8 (a) UV-vis spectrum and (b) ESI-MS of **Au_{22}-L^4**. Inset shows the experimental (black) and calculated (red) isotopic patterns of the main peak. CsOAc was added to enhance the ionization of the neutral nanoclusters.

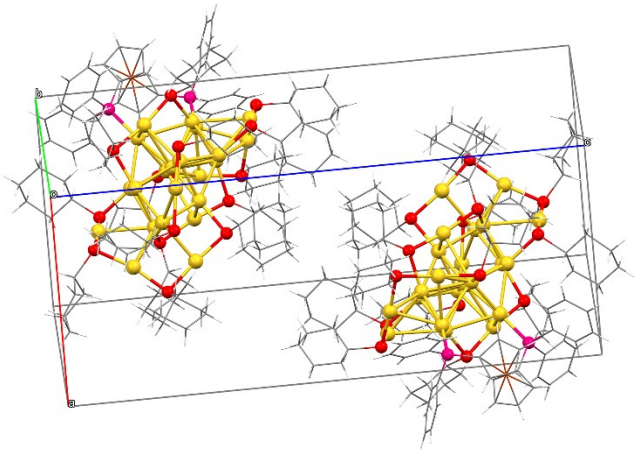

Fig. S9 A unit cell of the **Au_{22}-DPPF** crystal. (Labels: golden = Au; red = S; magenta = P; gray = C; white = H.).

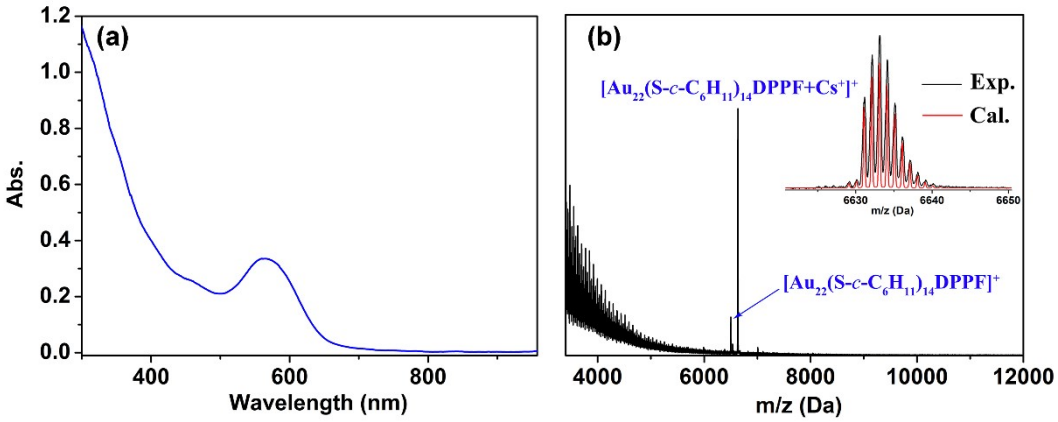

Fig. S10 ESI-MS of **Au_{22}-DPPF**. Inset shows the experimental (black) and calculated (red) isotopic patterns of the main peak.

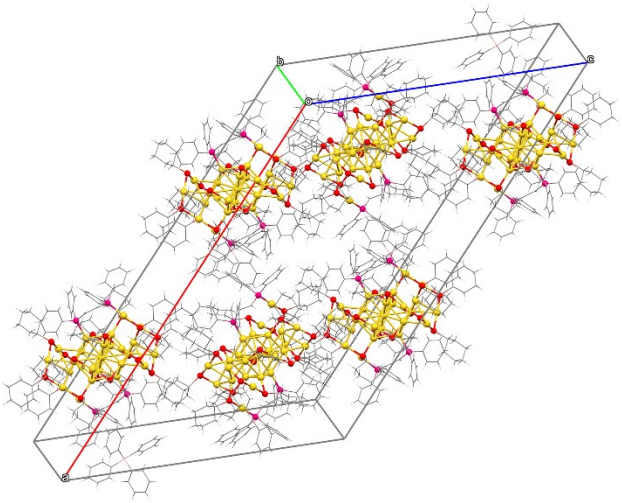

Fig. S11 A unit cell of the **Au_{25}-TDPE** crystal. (Labels: golden = Au; red = S; magenta = P; gray = C; white = H.).

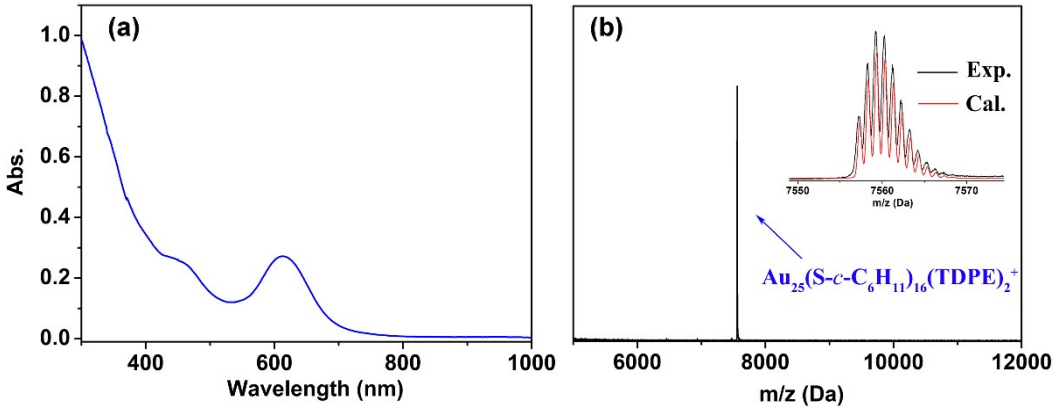

Fig. S12 (a) UV-vis spectrum and (b) ESI-MS of **Au_{25}-TDPE**. Inset shows the experimental (black) and calculated (red) isotopic patterns of the main peak.

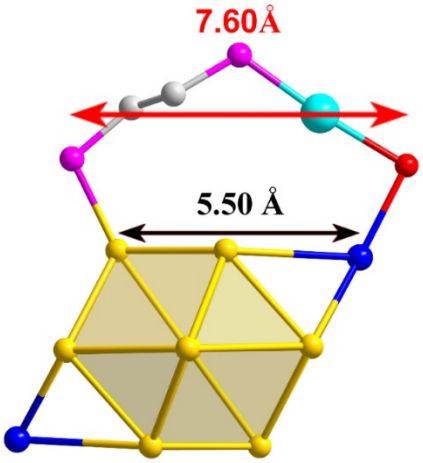

Fig. S13 The P−S distance (indicated with red arrow) and Au−Au distance (indicated with black arrow) at the binding site of TDPE in the **Au_{25}-TDPE**. (Labels: sky blue, blue, golden = Au; red = S; magenta = P; gray = C.)

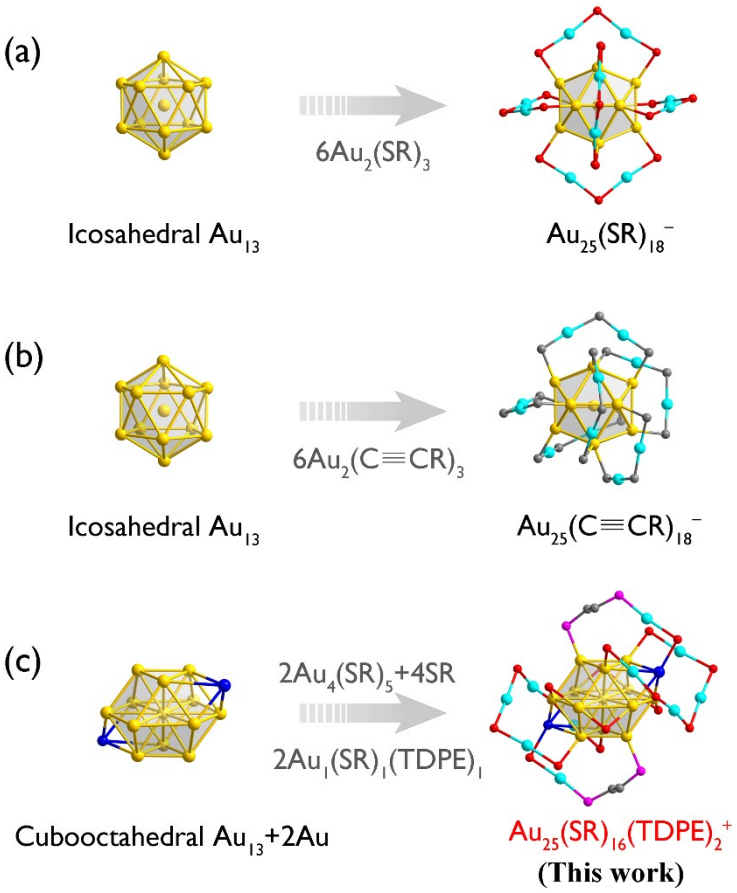

Fig. S14 Comparison of the inner cores and structural frameworks of three Au_{25} nanoclusters exhibiting 8 e^-. (a) $Au_{25}(SR)_{18}^-$ consisted of an icosahedral Au_{13} kernel and six $Au_2(SR)_3$ motifs;[2,3] (b) $Au_{25}(C{\equiv}CR)_{18}^-$ consisted of an icosahedral Au_{13} kernel and six $Au_2(C{\equiv}CR)_3$ motifs (For showing the surface motifs more clearly, one of the carbon atoms in the alkyne group is omitted);[4] (c) $Au_{25}(SR)_{16}(TDPE)_2^+$ consisted of a Au_{15} kernel (cubooctahedral Au_{13} added with two gold atoms) two $Au_4(SR)_5$, four bridging -SR and two $Au_1(SR)_1(TDPE)_1$ motifs. (Labels: sky blue, blue, golden = Au; red = S; magenta = P; gray = C.)

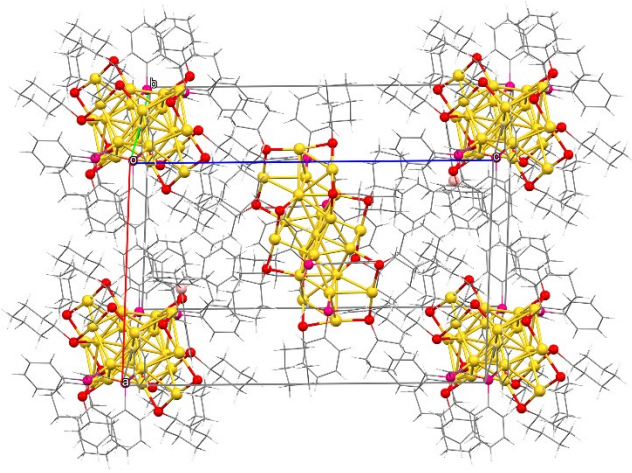

Fig. S15 A unit cell of the **Au_{21}-CDPE** crystal. (Labels: golden = Au; red = S; magenta = P; gray = C; white = H.)

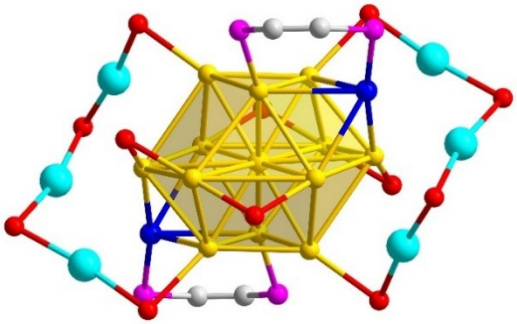

Fig. S16 Crystal structure of **Au_{21}-CDPE**. All of the H atoms and most of the carbon atoms are omitted. (Labels: sky blue, blue, golden = Au; red = S; magenta = P; gray = C.)

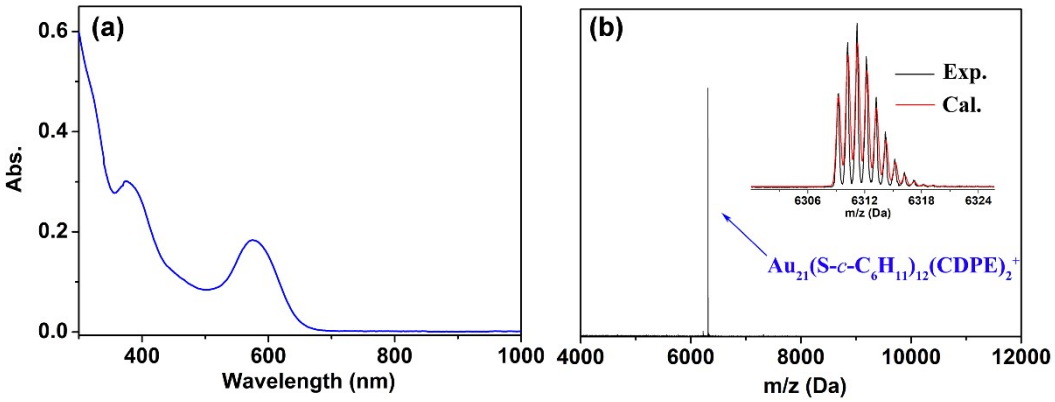

Fig. S17 (a) UV-vis spectrum and (b) ESI-MS of **Au_{21}-CDPE**. Inset shows the experimental (black) and calculated (red) isotopic patterns of the main peak.

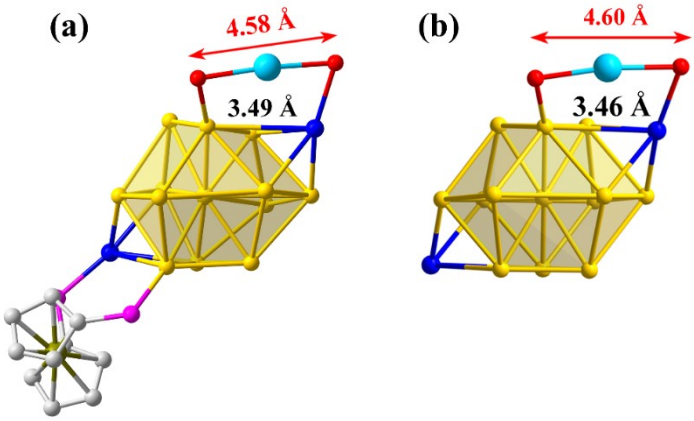

Fig. S18 Comparison of the S−S distance and Au−Au distance at the Au_1S_2 binding site in (a) **Au_{22}-DPPF** and (b) $Au_{23}(SR)_{16}^-$. (Labels: sky blue, blue, golden = Au; red = S; magenta = P; olive = Fe, gray = C.)

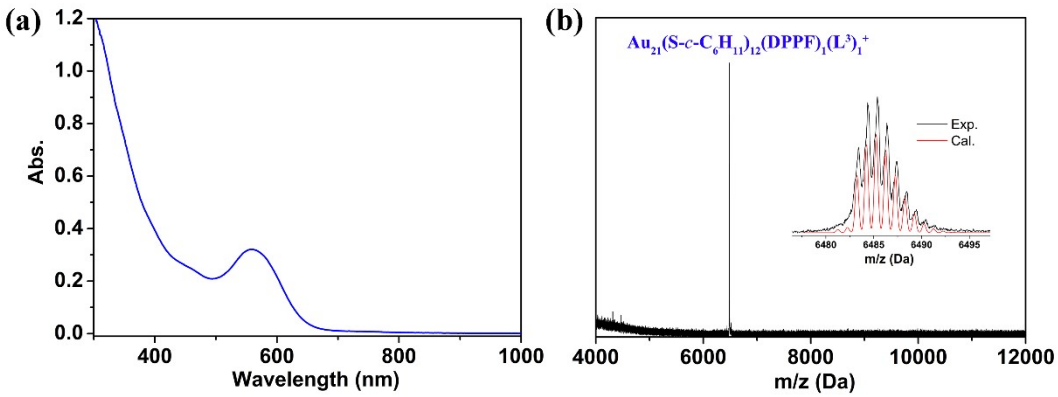

Fig. S19 (a) UV-vis spectrum of **Au_{21}-DPPF-L^3** (b) ESI-MS of **Au_{21}-DPPF-L^3**. Inset shows the experimental (black) and calculated (red) isotopic patterns of the main peak.

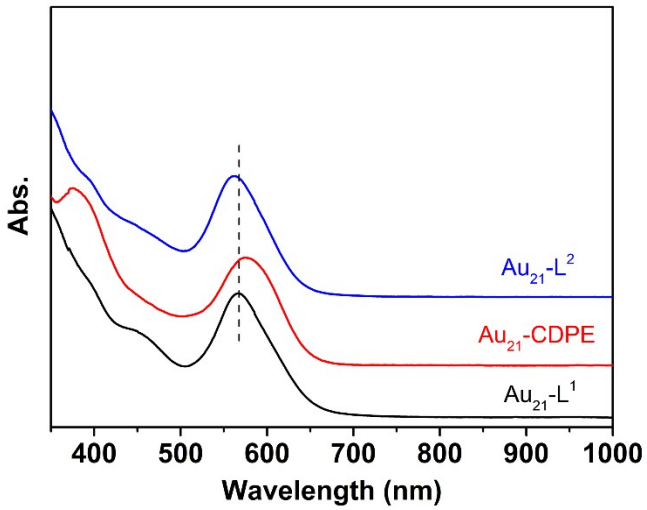

Fig. S20 UV-vis spectra of **Au_{21}-L^1**, **Au_{21}-CDPE** and **Au_{21}-L^2**. The dash line indicates the position of the absorption wavelength of **Au_{21}-L^1**.

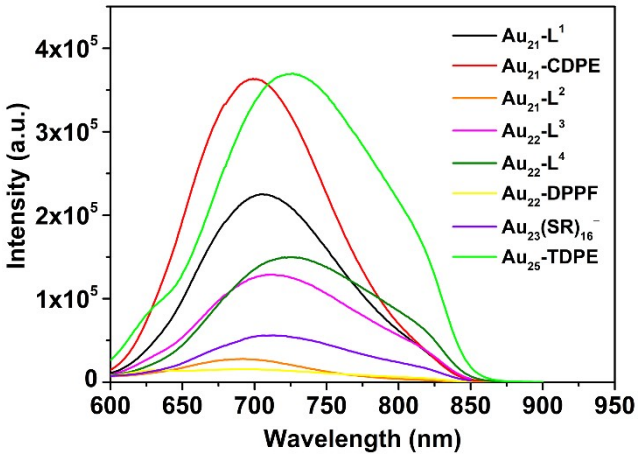

Fig. S21 Comparison of the photoluminescence of different Au NCs.

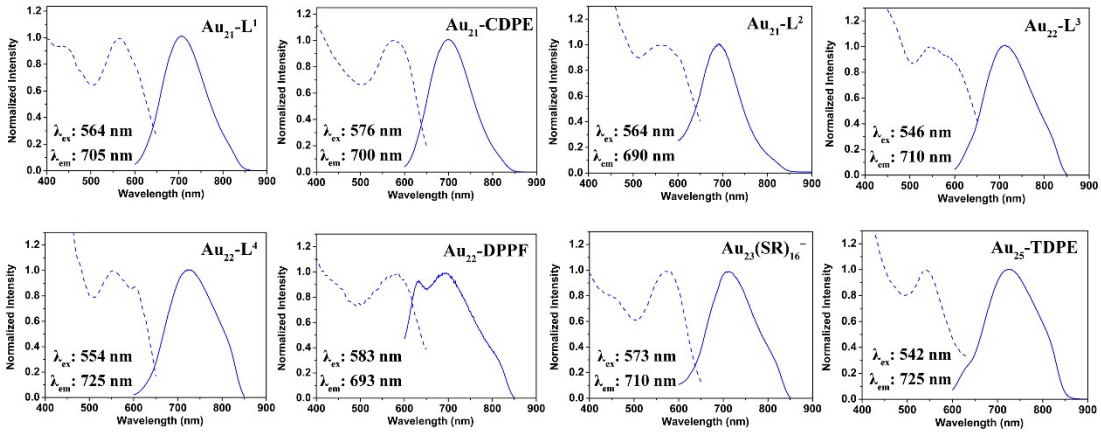

Fig. S22 Excitation spectra (dash line) and emission spectra (solid line) of the Au NCs in this study. (λ_{ex}: excitation wavelength; λ_{em}: emission wavelength)

2. Supporting Tables

Table S1. Crystal data and structure refinement for **Au_{21}-L^2**.

CCDC code	2119766
Empirical formula	$C_{124}H_{180}Au_{21}P_4S_{12}$
Formula weight	6315.57
Temperature/K	150
Crystal system	triclinic
Space group	P-1
a/Å	15.4160(9)
b/Å	15.9669(11)
c/Å	19.0841(12)
α/°	111.495(5)
β/°	112.712(5)
γ/°	93.327(5)
Volume/Å^3	3921.4(5)
Z	1
ρ_{calc}g/cm^3	2.674
μ/mm^{-1}	38.030
F(000)	2835.0
Crystal size/mm^3	0.1 × 0.05 × 0.02
Radiation	CuKα (λ = 1.54186)
2Θ range for data collection/°	8.216 to 129.996
Index ranges	$-8 \le h \le 18$, $-16 \le k \le 18$, $-22 \le l \le 19$
Reflections collected	25826
Independent reflections	12772 [R_{int} = 0.0556, R_{sigma} = 0.0792]
Data/restraints/parameters	12772/373/727
Goodness-of-fit on F^2	0.930
Final R indexes [I>=2σ (I)]	R_1 = 0.0607, wR_2 = 0.1467
Final R indexes [all data]	R_1 = 0.0767, wR_2 = 0.1524
Largest diff. peak/hole / e Å^{-3}	3.19/-4.59

Table S2. Crystal data and structure refinement for **Au_{22}-L^3**.

CCDC code	2119770
Empirical formula	$C_{112}H_{182}Au_{22}Cl_2P_2S_{14}$
Formula weight	6443.51
Temperature/K	120
Crystal system	orthorhombic
Space group	$Pca2_1$
a/Å	33.411
b/Å	16.475

c/Å	54.849
α/°	90
β/°	90
γ/°	90
Volume/Å^3	30191.6
Z	8
ρ_{calc}g/cm^3	2.835
μ/mm^{-1}	41.649
F(000)	23040.0
Crystal size/mm^3	0.1 × 0.1 × 0.01
Radiation	CuKα (λ = 1.54186)
2Θ range for data collection/°	7.708 to 119.99
Index ranges	-15 ≤ h ≤ 37, -18 ≤ k ≤ 15, -31 ≤ l ≤ 61
Reflections collected	54187
Independent reflections	28723 [R_{int} = 0.0799, R_{sigma} = 0.0750]
Data/restraints/parameters	28723/2873/2642
Goodness-of-fit on F^2	1.047
Final R indexes [I>=2σ (I)]	R_1 = 0.1146, wR_2 = 0.2797
Final R indexes [all data]	R_1 = 0.1443, wR_2 = 0.3253
Largest diff. peak/hole / e Å^{-3}	5.67/-3.10

Table S3. Crystal data and structure refinement for **Au_{22}-DPPF**.

CCDC code	2119769
Empirical formula	$C_{120}H_{186}Au_{22}Cl_4FeP_2S_{14}$
Formula weight	6670.37
Temperature/K	120
Crystal system	triclinic
Space group	P-1
a/Å	15.8416(5)
b/Å	17.5548(5)
c/Å	29.6424(8)
α/°	80.682(2)
β/°	82.909(2)
γ/°	63.942(2)
Volume/Å^3	7295.0(4)
Z	2
ρ_{calc}g/cm^3	3.037
μ/mm^{-1}	44.222
F(000)	5984.0
Crystal size/mm^3	0.05 × 0.05 × 0.01

Radiation	CuKα (λ = 1.54186)
2Θ range for data collection/°	7.766 to 129.996
Index ranges	$-18 \leq h \leq 18$, $-13 \leq k \leq 20$, $-34 \leq l \leq 34$
Reflections collected	49548
Independent reflections	23672 [R_{int} = 0.0844, R_{sigma} = 0.1039]
Data/restraints/parameters	23672/849/1486
Goodness-of-fit on F^2	0.950
Final R indexes [I>=2σ (I)]	R_1 = 0.0679, wR_2 = 0.1725
Final R indexes [all data]	R_1 = 0.1018, wR_2 = 0.1891
Largest diff. peak/hole / e Å^{-3}	3.02/-2.67

Table S4. Crystal data and structure refinement for **Au_{25}-TDPE**.

CCDC code	2119767
Empirical formula	$C_{172}H_{240}Au_{25}BP_4S_{16}$
Formula weight	7879.44
Temperature/K	120
Crystal system	monoclinic
Space group	C2/c
a/Å	49.7888(10)
b/Å	17.4433(4)
c/Å	31.9121(9)
α/°	90
β/°	129.254(2)
γ/°	90
Volume/Å^3	21461.1(10)
Z	4
ρ_{calc}g/cm^3	2.439
μ/mm^{-1}	33.236
F(000)	14272.0
Crystal size/mm$_3$	0.1 × 0.05 × 0.02
Radiation	CuKα (λ = 1.54186)
2Θ range for data collection/°	12.394 to 139.308
Index ranges	$-55 \leq h \leq 60$, $-12 \leq k \leq 21$, $-35 \leq l \leq 38$
Reflections collected	44862
Independent reflections	19420 [R_{int} = 0.0587, R_{sigma} = 0.1037]
Data/restraints/parameters	19420/707/952
Goodness-of-fit on F^2	0.872
Final R indexes [I>=2σ (I)]	R_1 = 0.0447, wR_2 = 0.0986
Final R indexes [all data]	R_1 = 0.0819, wR_2 = 0.1152
Largest diff. peak/hole / e Å^{-3}	2.30/-1.77

Table S5. Crystal data and structure refinement for **Au_{21}-CDPE**.

CCDC code	2119768
Empirical formula	$C_{148}H_{196}Au_{21}BP_4S_{12}$
Formula weight	6630.74
Temperature/K	120
Crystal system	triclinic
Space group	P-1
a/Å	17.4996(2)
b/Å	21.3266(3)
c/Å	26.0965(4)
α/°	69.4100(10)
β/°	83.6220(10)
γ/°	74.5830(10)
Volume/Å^3	8787.5(2)
Z	2
ρ_{calc}g/cm^3	2.506
μ/mm^{-1}	33.992
F(000)	6000.0
Crystal size/mm^3	0.05 × 0.05 × 0.04
Radiation	CuKα (λ = 1.54186)
2Θ range for data collection/°	9.138 to 124.998
Index ranges	$-20 \le h \le 9$, $-24 \le k \le 24$, $-28 \le l \le 30$
Reflections collected	49686
Independent reflections	26740 [R_{int} = 0.0399, R_{sigma} = 0.0392]
Data/restraints/parameters	26740/1195/1666
Goodness-of-fit on F^2	1.034
Final R indexes [I>=2σ (I)]	R_1 = 0.0637, wR_2 = 0.1766
Final R indexes [all data]	R_1 = 0.0712, wR_2 = 0.1865
Largest diff. peak/hole / e Å^{-3}	4.42/-4.85

3. References

1. M. Zhu, C. M. Aikens, F. J. Hollander, G. C. Schatz and R. Jin, *J. Am. Chem. Soc.*, 2008, **130**, 5883.

2. M. W. Heaven, A. Dass, P. S. White, K. M. Holt and R. W. Murray, *J. Am. Chem. Soc.*, 2008, **130**, 3754.

3. J.-J. Li, Z.-J. Guan, Z. Lei, F. Hu and Q.-M. Wang, *Angew. Chem., Int. Ed.*, 2019, **58**, 1083.